Icelike Melting of Hexagonal Columnar Crystals

Shilpa Jain and David R. Nelson*

Lyman Laboratory of Physics, Harvard University, Cambridge, Massachusetts 02138

Received June 11, 1996; Revised Manuscript Received September 30, 1996[⊗]

ABSTRACT: We study the possibility of reentrant melting of a hexagonal columnar crystal of flexible charged polymers at high enough densities. The Lindemann criterion is employed in determining the melting point. Lattice fluctuations are calculated in the Debye model, and an analogy with the Abrikosov vortex lattice in superconductors is exploited in estimating both the elastic constants of the hexagonal lattice and the appropriate Lindemann constant. We also discuss the unusual functional integral describing the statistical mechanics of a single polymer in an Einstein cage model using the path-integral formulation. A crossover as a function of an external field along the column axis is also discussed.

I. Introduction

Liquid crystals have generated much interest due to the variety of phase structures they exhibit, not all of which are completely understood. In this paper, we focus our attention on flexible chains of polyelectrolytes that are known to form hexagonal columnar crystals at the ordered end of their phase sequence, i.e., at high densities. Most biopolymers fall in this category, e.g., DNA, xanthan, and PBLG when dissolved in suitable solvents[1] which are aqueous salt solutions in most cases. These materials are crystalline only in the two directions perpendicular to the polymer strands; the sequences of monomers in adjacent strands are not in registry. Owing to their limited temperature range of stability, the phase transitions are usually achieved by changing the density of polymers ρ and the ion concentration c in the solution. The gas of ions screens the otherwise long-range Coulomb repulsion between the ionized polymers, resulting in an exponentially decaying interaction for distances greater than the Debye−Hückel screening length $\lambda_D \equiv \kappa_D^{-1} \propto c^{-1/2}$.[2]

In this paper we explore the possibility of the columnar crystal melting with increasing densities or osmotic pressures, similar to the melting of ice at high pressure or to the melting of quantum Wigner crystals at high densities.

Our motivation is an analogy with the melting of the Abrikosov flux lattice in type II superconductors at high magnetic fields H. The flux lines also form a hexagonal columnar crystal, which was earlier thought to exist throughout the entire region between the upper and lower critical fields $H_{c_1}(T) < H < H_{c_2}(T)$. It has, however, been predicted[3] and recently experimentally verified[4] that the flux crystal melts into an entangled vortex liquid via a first-order phase transition as the vortex density is increased. The melted flux liquid phase is *denser* than the coexisting vortex crystal, consistent with the negative slope of the melting line $H_m(T)$ and the Clausius−Clapeyron equation. The flux segments interact with a screened-Coulomb-like repulsion, similar to that between the polyelectrolytes, the role of the screening length λ_D being played by the London penetration depth λ. Although there are also significant differences between the two cases, we believe thermal undulations of ordered hexagonal columnar polyelectrolytes in the soft interaction potential they experience at low screening can lead to anomalous icelike melting just as for the flux lattice. Experimentally, a reentrant "disordered phase" has been observed by Fraden[5] in flexible fd bacteriophages at densities beyond the crystalline phase, although the relation of this phase to the dense liquid we predict here is not yet clear.

In trying to estimate when the columnar crystalline phase would melt, we have applied the Lindemann criterion which predicts melting when the root mean square thermal phonon displacements exceed a certain fraction of the lattice spacing, known as the Lindemann constant c_L. Although c_L for polymer columnar crystals has not yet been measured directly, Odijk[6] has attempted to calculate it from an approximate low-density melting curve by estimating the fluctuations analytically. He found a c-dependent value of c_L in the high-c regime with an average value around 0.126 which could be larger if the melting data were more precise. Here we have borrowed its value from experiments on the Abrikosov flux crystal ($c_L \approx 0.15$).[7]

Although we focus here on flexible polymers with relatively long-range electrostatic interactions, the same methods may be applied to other regimes and systems. For example, if a strong magnetic or electric field is used to ensure alignment of the polymers, it may be possible to dilute the columnar hexagonal phase until the repulsive electrostatic interactions are in the weak exponentially screened regime. Melting into liquid of aligned polymers will now occur upon sufficient *dilution*, similar to predictions for vortex lines at low magnetic fields. Where this low-density melting occurs can also be estimated via a Lindemann criterion. One can as well use the Lindemann criterion to treat melting of hexagonal columnar phases composed of disklike molecules instead of polymers. All that is required is knowledge of the elastic constants such as those entering eqs 4.3 and 4.4 below. For an alternative approach which leads to phase diagrams for hexagonal columnar phases dominated by hard-core excluded volume interactions, see Selinger and Bruinsma.[8]

In the following section, we review a simple calculation[9] that uses dimensional analysis to estimate the fluctuations of a single polymer under the influence of its neighbours, as in the Einstein "particle in a cage" model of phonons in atomic crystals. Section III describes the statistical mechanics of long polymers in a cylindrical cage in more detail, by mapping onto the problem of the two-dimensional "quantum mechanics" of a particle in a potential, with, however, an acceleration-dependent "kinetic energy" term. The model and the analysis presented in these sections are similar to

[⊗] Abstract published in *Advance ACS Abstracts,* November 1, 1996.

S0024-9297(96)00848-0 CCC: $12.00

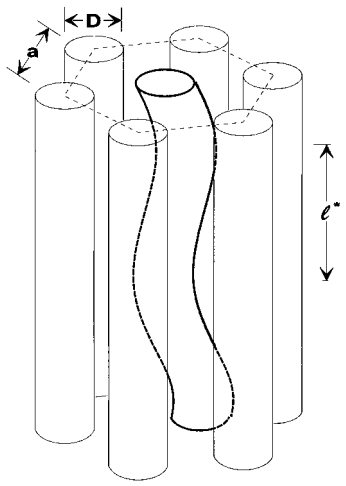

Figure 1. In the "polymer in a cage" model, each polymer is viewed as fluctuating in the "cage" formed by the potential field of its neighbors.

those of Podgornik and Parsegian,[2] whose calculations (which rely on analogy with conventional quantum mechanics) are, however, better suited to crystals in a strong external electric or magnetic field. On the other hand, the model with the bending term has been analyzed in detail by Burkhardt[10] in the absence of external fields and by Kleinert[11] and Dodonov *et al.*[12] In Appendix A we outline the calculations relevant to our problem and extract the results that are discussed in section III. Improvement on the Einstein model requires collective treatment of the lattice fluctuations as in the Debye model of phonons in conventional solids, described in section IV. Appendix B presents a numerical study of the validity of the harmonic approximation.

II. "Polymer in a Cage" Model

In the Einstein model, each polymer in the crystalline phase sits in a potential "cage" formed by the surrounding polymers, fluctuating around the potential minimum (see Figure 1).[2] The fluctuations are determined by the bending rigidity κ of the polymer and the form of the potential well. The rigidity κ is related to the persistence length l_P of the polymer in dilute solution at that temperature: $l_P = \kappa/T$ is the length a free polymer would wander before bending appreciably (we use units such that $k_B = 1$). However, in the crystal its wanderings are more confined, with the potential typically deflecting it back into its cage before it can bend appreciably.

The potential energy per unit length of a polymer due to interactions with a perfectly straight neighboring polymer at a distance r is[2]

$$V(r) = 2u_o K_0(\kappa_D r) \tag{2.1}$$

The prefactor is given by $u_o/T = l_B/b^2\gamma$, where l_B is the Bjerrum length $e^2/\epsilon T$ in the solution, b is the distance per unit charge (screened by counterions) along the polymer, and γ is a factor that accounts for the finite thickness of the polymer, $\gamma \approx \kappa_D(D/2)K_1(\kappa_D D/2)$, D being the hard core diameter of the polymer. Here e is the electron charge and ϵ is the dielectric constant of the solvent. This form of the potential assumes that r is large enough that $V(r)b \ll T$, which, for $\kappa_D r \ll 1$, requires that $b \gg l_B$, that is, the polymer be weakly charged. For a detailed discussion of corrections to the potential for DNA, see Schellman and Stigter.[13]

For fluctuating polymers, we can still use eq 2.1 as a reasonable approximation if the fluctuations are a small fraction of the lattice spacing a, and the slopes relative to the average direction of alignment (say, $\hat{\mathbf{z}}$) are small.

Let the planar coordinate $\mathbf{r}(z) \perp \hat{\mathbf{z}}$ describe the trajectory of a polymer. If the surrounding polymers sit at lattice sites $\mathbf{R}_\nu$ (with lattice constant a), the potential minimum they create is, on average, along the line $\mathbf{r}(z) = \mathbf{0}$, and the potential energy for a small displacement $\mathbf{r}$ is

$$U(\mathbf{r}) \simeq U(\mathbf{0}) + \frac{1}{2}k\mathbf{r}^2 \tag{2.2}$$

where

$$k = \frac{1}{2}\sum_{\mathbf{R}_\nu}\left[\frac{V'(R_\nu)}{R_\nu} + V''(R_\nu)\right]$$

$$= u_o\kappa_D{}^2\sum_{\mathbf{R}_\nu \neq \mathbf{0}} K_0(\kappa_D R_\nu) \tag{2.3a}$$

The two terms in k correspond respectively to displacements $\mathbf{r}$ perpendicular and parallel to $\mathbf{R}_\nu$, and the factor of $^1/_2$ comes from directional averaging. In the last line, we have used eq 2.1 and the differential equation which defines the modified Bessel function K_0.[14] A mean field-like treatment[15] would increase the effective k by $O(\exp(\kappa_D{}^2\langle|\mathbf{r}|^2\rangle))$, which can be ignored if $\kappa_D d \ll 1$, $d = \langle|\mathbf{r}|^2\rangle^{1/2} < c_L a$. When $\kappa_D a \ll 1$, we approximate the sum by an integral, $\sum_{\mathbf{R}_\nu \neq 0} \rightarrow \rho \int d^2\mathbf{r}$ where $\rho = 2/\sqrt{3}a^2$ is the areal density of polymers, and find

$$k \approx \frac{4\pi}{\sqrt{3}}\frac{u_o}{a^2} \qquad (\kappa_D a \ll 1) \tag{2.3b}$$

We can now write the fluctuation energy of the polymer approximately as

$$\delta E[\mathbf{r}(z)] = E[\mathbf{r}(z)] - U(\mathbf{0}) = \int_0^L dz\left[\frac{1}{2}\kappa\left(\frac{d^2\mathbf{r}}{dz^2}\right)^2 + \frac{1}{2}k\mathbf{r}^2\right] \tag{2.4}$$

where L is the sample length along $\hat{\mathbf{z}}$ and the integral is over z rather than the polymer contour length, an approximate simplification provided that the slopes $|d\mathbf{r}/dz|$ are small.

Dimensional analysis gives the characteristic length scale for fluctuations:

$$l^* \approx \left(\frac{\kappa}{k}\right)^{1/4} \tag{2.5}$$

which is the analogue for a harmonic potential of Odijk's deflection length l_{def}.[16] The energy of a fluctuation of length l^* is $E^* \approx \kappa^{1/4}k^{3/4}|\mathbf{r}|^2$. Assuming that segments of length l^* fluctuate independently and applying the equipartition theorem, we obtain

$$d \equiv \langle|\mathbf{r}|^2\rangle \approx \frac{T}{\kappa^{1/4}k^{3/4}} \tag{2.6}$$

up to factors of $O(1)$. Note that these quantities satisfy the relation $l_{def} \approx l_P{}^{1/3}d_{eff}{}^{2/3}$ derived by Odijk for the case of hard-core interactions, if we replace the effective hard-core diameter d_{eff} of the confining tube with d.

For $\kappa_D a \gg 1$, k decays exponentially with $\kappa_D a$ and the fluctuations increase exponentially, eventually destroy-

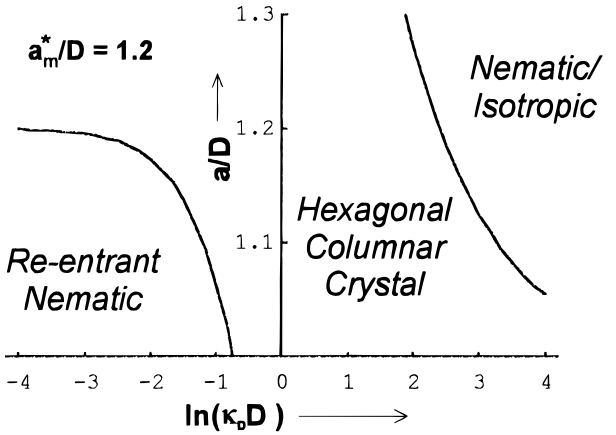

Figure 2. Schematic phase diagram of the polyelectrolytes in terms of lattice constant a and Debye screening length κ_D, scaled with respect to the polymer hard core diameter D which appears in the interaction strength u_o through a factor accounting for finite polymer thickness. The lines indicate melting of the columnar crystalline phase, as obtained from the Lindemann criterion for $\kappa_D a_m < 1/10$ (reentrant melting) and >10 (melting to a nematic or isotropic phase), taking the $\kappa_D a_m \to 0$ limit of a_m/D (which is independent of κ_D) to be 1.2 (for reentrant melting to be observable, this has to be >1).

ing in-plane long-range order, so that at low densities one has the expected melting to a nematic or isotropic phase, with liquidlike in-plane order.

However, for $\kappa_D a \ll 1$, $k \propto 1/a^2$ from eq 2.3b, and we find

$$\frac{\langle|\mathbf{r}|^2\rangle}{a^2} \propto \frac{1}{a^{1/2}} \tag{2.7}$$

so that for very high densities also, fluctuations increase relative to the lattice spacing, in this case due to confinement of a flexible line by a soft potential ($\sim\log r$). Thus, the crystalline state is not viable at high densities and should melt, presumably into an entangled polymer nematic. As discussed by one of us, similar icelike melting arises at high densities for all repulsive power-law potentials $V(r) \sim 1/r^n$ provided $n < 2/3$.[17]

The locus of the critical lattice constant for melting a_m, as a function of ionic strength (via κ_D), temperature, etc. is given by solving the self-consistent equation:

$$\frac{T}{\kappa^{1/4} k(a_m)^{3/4} a_m^{\,2}} \approx c_L^{\,2} \tag{2.8}$$

where $k(a_m)$ is given by eq 2.3a. It yields two melting lines—a $\kappa_D a_m \gg 1$ melting to a nematic or isotropic phase and a $\kappa_D a_m \ll 1$ reentrant melting, as illustrated in Figure 2. In terms of dimensionless variables $x \equiv \kappa_D D$, $y \equiv a_m/D$, and $A \equiv a_m^*/D$, where a_m^* is the solution of the above equation in the $\kappa_D a_m \to 0$ limit and D is the hard-core diameter of the polymer, entering the calculations through the interaction strength u_o, which determines k, the reentrant melting line is given by

$$y \approx A\left[\frac{x}{2}K_1\left(\frac{x}{2}\right)\right]^3 \tag{2.9a}$$

while the low-density melting line is given by

$$\frac{y^{8/3}K_o''(xy)}{K_1(x/2)^2} \approx \frac{A^{2/3}}{6} \tag{2.9b}$$

which should, however, be corrected for undulation-enhanced electrostatic repulsion[15] if $\kappa_D^2\langle|\mathbf{r}|^2\rangle$ is not small. The numerical coefficients here have been obtained by using the results of section IV. The observability of reentrant melting at high densities requires $A > 1$.

This crude derivation has also assumed that the slopes $\sim d/l^* \ll 1$. If the deflection length is of the order of the fluctuation size, then we might no longer have a soft loglike potential for $a \ll \lambda_D$: interactions would look more 3-dimensional, that is, more like $1/r$, and this would suppress the fluctuations at small a, suppressing the transition.

The small slopes condition was also used to replace the polymer contour length s with distance along the axis z. The correction for this approximation would involve replacing dz with $dz(1 + |d\mathbf{r}/dz|^2)$ to lowest order in $|d\mathbf{r}/dz|$. This would give rise to an additional quadratic term $^1/_2 g(d\mathbf{r}/dz)^2$ in $\delta E[\mathbf{r}(z)]$, where

$$g = U(\mathbf{0}) = \sum_{\mathbf{R}_\nu \neq 0} 2u_o K_0(\kappa_D R_\nu) = 2k/\kappa_D^{\,2}$$

This correction can be neglected if $\lambda_D \ll l^*$, so that each deflection segment acts as a straight rod with respect to the interaction.

III. Statistical Mechanics of a Polymer in a Quadratic Potential

The statistical mechanics associated with the Gaussian model (2.4) can in fact be computed exactly.[10−12] The approximation that the polymer fluctuates freely in a quadratic potential requires a distribution in $\mathbf{r}$ with a spread small enough so that anharmonicities associated with the boundaries of the cage are negligible. (This approximation has been investigated numerically for polymer parameters corresponding to B-DNA in Appendix B.) The statistical mechanics is governed by the partition function

$$Z = \int D\mathbf{r}(z) e^{-\delta E[\mathbf{r}(z)]/T} \equiv e^{-\delta F/T} \tag{3.1}$$

The problem can be mapped onto that of a 2D particle in a potential, obeying unusual "soft" imaginary quantum mechanics (see Appendix A), so termed because the energy of long-wavelength fluctuations with wavevector q along the z-direction scales as q^4 rather than as q^2, which is the case for the more common problems representing a string under tension that map onto regular quantum mechanics. If the head−tail unbinding transition[9] does not occur before melting, finite length polymers will be connected head-to-tail across the sample and it is appropriate to take the limit $L \to \infty$, the thermodynamic properties of the polymer can then be extracted from the ground state of this "soft" quantum mechanics problem.

We consider the general energy function

$$\delta E[\mathbf{r}(z)] = \int_0^L dz \left[\frac{1}{2}\kappa\left(\frac{d^2\mathbf{r}}{dz^2}\right)^2 + \frac{1}{2}g\left(\frac{d\mathbf{r}}{dz}\right)^2 + \frac{1}{2}k\mathbf{r}^2\right] \tag{3.2}$$

g representing the coupling to an external magnetic field $\mathbf{H} = H\hat{\mathbf{z}}$: $g = \chi_a H^2 \rho$ where χ_a is the anisotropic bulk magnetic susceptibility of the polymer crystal. Unless $\lambda_D \ll l^*$, g should also include a term $2k/\kappa_D^2$ due to the inextensibility of the polymer, as explained at the end

of the previous section. As shown in Appendix A, we then find

$$f \equiv \delta F/L = T\sqrt{2\sqrt{\frac{k}{\kappa}} + \frac{g}{\kappa}} \equiv T/l^*\left(\frac{k}{\kappa},\frac{g}{\kappa}\right) \quad (3.3)$$

i.e., a purely entropic contribution reflecting the entropy reduction due to confinement.[18] Since equipartition holds exactly for a quadratic energy function, the total fluctuation energy is $\langle \delta E\rangle = TL/l_o$ (l_o = length of a monomer), making the total entropy per unit length

$$S/L = (\delta E - \delta F)/LT = 1/l_o - 1/l^* \quad (3.4)$$

This form for the entropy can be understood via a simple argument:

Let us, for convenience, discretize the motion of the polymer—at each step of length l_o, it can move into any of n neighboring lattice sites in the next plane. Let us suppose that when, after l_{def}/l_o such steps, it hits the wall of the confining tube, it has only $n' \approx n/2$ sites to move into. The entropy per unit length of a polymer of length L is then

$$S/L \approx \frac{1}{L}\ln[n^{L/l_o}/(n/n')^{L/l_{def}}]$$

$$\approx \frac{1}{l_o}\ln(n) - \frac{1}{l_{def}}\ln 2 \quad (3.5)$$

which looks very similar to expression 3.4 and suggests we interpret l^* as a deflection length.

For $H = 0 = g$, one finds an entropy reduction of 1 unit per length $l^*/\sqrt{2}$, confirming that l^* plays the role of a deflection length for a harmonic potential.

An experimental probe into the free energy per unit length $F(a)/L = U(\mathbf{0}) + T/l^*$ is provided by measurements of the expansive force per unit length of the crystal using osmotic stress techniques.[2,19] Since for $\kappa_D a \gg 1$, $U(\mathbf{0})$, $k \propto K_0(\kappa_D a)$, and $K_0(\kappa_D a) \sim e^{-\kappa_D a}$, we infer from eq 3.3 that the force $\propto \partial F(a)/\partial a$ should exhibit an exponential decay length at large a 4 times that at smaller a, while in the presence of a strong enough magnetic field, it should only be doubled, the crossover occurring around $g = 2\sqrt{\kappa k}$.

The fluctuations $\langle|\mathbf{r}|^2\rangle \equiv \langle\int_0^L dz\ \mathbf{r}^2(z)\rangle/L$ can be calculated as (see Appendix A)

$$\langle|\mathbf{r}|^2\rangle = 2\frac{\partial f}{\partial k} = \frac{T}{\sqrt{k(2\sqrt{\kappa k} + g)}} \quad (3.6)$$

and for $H = 0 = g$, eq 2.6 is recovered up to numerical factors.

IV. Phonon Fluctuations

Having obtained a rough estimate of the fluctations by looking at a single polymer, we now proceed to a more rigorous "Debye" treatment of the lattice fluctuations by integrating over the phonon modes in a continuum description of the crystal. We introduce a 2D continuum phonon displacement field

$$\mathbf{u}(\mathbf{r},z) = \rho^{-1}\sum_i \mathbf{u}_i(z)\delta^{(2)}(\mathbf{r}_i - \mathbf{R}_i - \mathbf{u}_i(z)) \quad (4.1)$$

where $\mathbf{u}_i(z)$ is the displacement of the ith polymer from its equilibrium position $\mathbf{R}_i$ on a triangular lattice, and $\rho = 2/\sqrt{3}a^2$ is the average planar number density of the polymers that is fixed by, e.g., an external chemical potential or osmotic pressure. The average local nematic order parameter $\hat{\mathbf{n}} \equiv (n_z \approx 1, \mathbf{n}_\perp = \delta\mathbf{n})$, $|\delta\mathbf{n}| \approx d/l^* \ll 1$, is related to $\mathbf{u}$ by $\delta\mathbf{n} = \partial\mathbf{u}/\partial z$ in the continuum description.

Following earlier works,[8,9] we write the continuum free energy of the crystal as a sum of two parts:

$$F = F_{nematic} + F_{crystal} \quad (4.2)$$

where

$$F_{nematic} = \frac{1}{2}\int dz \int d^2\mathbf{r}\,[K_1(\nabla_\perp\cdot\delta\mathbf{n})^2 + K_2(\nabla_\perp \times \delta\mathbf{n})^2 + K_3(\partial_z\delta\mathbf{n})^2] \quad (4.3)$$

K_1, K_2, and K_3 are the splay, twist, and bend Frank constants, respectively, of the polymer nematic with areal density ρ, and the elastic energy due to the hexagonal columnar phase is

$$F_{crystal} = \int dz \int d^2\mathbf{r}\left[\mu\, u_{ij}^2 + \frac{1}{2}\lambda\, u_{kk}^2\right] \quad (4.4)$$

where $u_{ij} = (\partial_i u_j + \partial_j u_i)/2$ is the linearized 2D strain field and μ and λ are the Lamé coefficients, determined by $V(r)$.

The mean square phonon displacement can be estimated using the equipartition theorem in Fourier space as

$$\langle|\mathbf{u}|^2\rangle = T\int\frac{d^2q_\perp}{(2\pi)^2}\int\frac{dq_z}{2\pi}\left[\frac{1}{K_3q_z^4 + K_2q_z^2q_\perp^2 + \mu q_\perp^2} + \frac{1}{K_3q_z^4 + K_1q_z^2q_\perp^2 + (\lambda+2\mu)q_\perp^2}\right] \quad (4.5)$$

$$\equiv \langle|\mathbf{u}_T|^2\rangle + \langle|\mathbf{u}_L|^2\rangle$$

a sum of transverse and longitudinal fluctuations.

The integral over q_z has an upper cutoff $\sim l_o^{-1}$, which can be extended to ∞ if $l_o \ll l^*$. The $q_\perp$ integral is over a hexagonal Brillouin zone, which for convenience, we can replace by a circle of the same area, so that its radius is $\Lambda_\perp = \sqrt{8\pi/\sqrt{3}}/a$.

The shear modulus $\mu \equiv c_{66}$ and the bulk modulus $(\lambda + \mu) \equiv c_{11} - c_{66}$ can be extracted from the analogy with the Abrikosov flux lattice.[20] Replacing the magnetic flux line density B/ϕ_o with ρ (ϕ_o = flux quantum $hc/2e$) and the London penetration depth λ with λ_D in the expressions for the elastic moduli obtained for the flux lattice,[20] we obtain

for $\kappa_D a \ll 1$,

$$c_{66} \approx \frac{1}{2\sqrt{3}}\frac{u_o}{a^2} \qquad c_{11}(\mathbf{q}_\perp) \approx \frac{4\pi u_o\rho^2}{\kappa_D^2 + q_\perp^2} \quad (4.6)$$

(When the interaction region of a polymer encompasses many polymers, a long-wavelength ($q_\perp \ll \kappa_D$) bulk strain causes a macroscopic change in this number, hence costing much more energy than a shear strain which preserves it ($\nabla\cdot\mathbf{u}_{shear} = 0$). At short wavelengths ($q_\perp \gg \kappa_D$), however, the number of polymers within the interaction range changes on the average by a factor $(\kappa_D/q_\perp)^2$ only, and the bulk modulus is smaller by that amount,

becoming comparable to the shear modulus.)

for $\kappa_D a \gg 1$,[21]

$$c_{66} \approx \frac{\sqrt{3}}{2} u_o \kappa_0''(\kappa_D a) \approx \frac{1}{2}\sqrt{\frac{3\pi}{2}} u_o \kappa_D{}^2 \frac{e^{-\kappa_D a}}{\sqrt{\kappa_D a}}$$

$$c_{11} \approx 3c_{66} \tag{4.7}$$

Thus, when the polymers are much farther apart than the interaction length, there is little distinction between a shear strain and a bulk strain and they are both small.

The bending Frank constant K_3 is easily seen to be $K_3 \approx \kappa\rho$, where $\kappa = Tl_P$. The other two Frank's constants are not as easy to estimate analytically. However, we do know that in most rigid nematics, they are of the same order of magnitude as K_3. For a semiflexible polymer, it might then be reasonable to assume that they are of the order of $Tl^*\rho$, since l^* is the length of effectively independently fluctuating segments. Therefore

$$\frac{K_{1,2}}{K_3} \approx \frac{l^*}{l_P} \tag{4.8}$$

which is typically $\ll 1$. A similar relation ($K_{1,2}/K_3 \approx \langle|\mathbf{u}|^2\rangle/l^{*2}$) was obtained by Selinger and Bruinsma[8] through dimensional analysis.

Integration of eq 4.5 gives

$$\frac{\langle|\mathbf{u}_T|^2\rangle}{a^2} = \frac{T}{2\pi c_{66}{}^{1/2} K_2{}^{1/2} a^2} \ln(\sqrt{1+\alpha_2} + \sqrt{\alpha_2}) \tag{4.9}$$

$\alpha_2 = \Lambda_\perp K_2/2\sqrt{K_3 c_{66}}$. With $K_2 \approx Tl^*\rho$ and $\kappa_D a \ll 1$, we find typically $\alpha_2 \ll 1$, so that eq 4.9 reduces to

$$\frac{\langle|\mathbf{u}_T|^2\rangle}{a^2} \approx \frac{T\Lambda_\perp{}^{1/2}}{\pi 2^{3/2} K_3{}^{1/4} c_{66}{}^{3/4} a^2}\left[1 + \frac{\alpha_2}{3} + ...\right] \tag{4.10}$$

same as eq 2.6 except for numerical factors.

Similarly, the longitudinal fluctuations for $\kappa_D a \gg 1$ are

$$\frac{\langle|\mathbf{u}_L|^2\rangle}{a^2} = \frac{T}{2\pi c_{11}{}^{1/2} K_1{}^{1/2} a^2} \ln(\sqrt{1+\alpha_1} + \sqrt{\alpha_1}) \tag{4.11}$$

$\alpha_1 = \Lambda_\perp K_1/2\sqrt{K_3 c_{11}}$. If $\alpha_{1,2} \ll 1$, $\langle|\mathbf{u}_L|^2\rangle \approx \langle|\mathbf{u}_T|^2\rangle/3^{3/4}$.

For $\kappa_D a \ll 1$,

$$\frac{\langle|\mathbf{u}_L|^2\rangle}{a^2} = \frac{T\Lambda_\perp}{4\pi\sqrt{4\pi u_o \rho^2 K_1} a^2} \int_0^1 dp \frac{(p^2+\delta^2)}{\sqrt{p^2(p^2+\delta^2) + 2p\sqrt{p^2+\delta^2}/\alpha'}} \tag{4.12}$$

where $\delta = \kappa_D a \ll 1$, and $\alpha' = \Lambda_\perp{}^2 K_1/\sqrt{4\pi u_o \rho^2 K_3}$, again typically $\ll 1$ if $K_1 \approx Tl^*\rho$. The integral 4.12 can then be expanded in α' as

$$\frac{\langle|\mathbf{u}_L|^2\rangle}{a^2} \approx \frac{T\Lambda_\perp{}^{1/2}}{4\pi 2^{3/2} K_3{}^{1/4} c_{11}{}^{3/4} a^2}\left[1 - \frac{\alpha'}{8} + ...\right] \tag{4.13}$$

similar to expression 4.10 for $\langle|\mathbf{u}_T|^2\rangle$. Because $c_{11}(q_\perp) \gg c_{66}$ for small $q_\perp$, $\langle|\mathbf{u}_L|^2\rangle$ is only about 6% of $\langle|\mathbf{u}_T|^2\rangle$, so $\langle|\mathbf{u}|^2\rangle \approx \langle|\mathbf{u}_T|^2\rangle$.

As a function of microscopic parameters, this yields the following melting point:

$$a_m \approx \frac{3^{3/4} b^3 [\kappa_D (D/2) K_1(\kappa_D D/2)]^3}{\pi^{3/2} 2^{1/2} l_B{}^{3/2} l_P{}^{1/2} c_L{}^4} \tag{4.14}$$

provided $a_m > D$. Note in particular that $a_m \equiv b^3$, $T^{3/2}$, $l_P{}^{-1/2}$. The persistence length l_P has some variation with temperature too. Fraden et al.[22] have observed a minimum in l_P at a certain temperature for the bacteriophage fd. The backbone length per unit electronic charge, b, is also a function of the salt concentration c,[2] as ion-binding to the polymer neutralizes some of its charge. As $c \to 0$, b should approach its bare value. In general, condition 4.14 requires that the polymer be flexible and weakly charged, though still be able to form a crystalline phase. To find a material with the optimum parameters may require some experimentation.

V. Conclusion

We have presented arguments for reentrant melting of a columnar crystal of flexible chains under conditions of high density when the columnar geometry is expected to lead to a soft interaction potential, allowing for the destruction of crystalline order with *increasing* density, similar to ice. Although the particular form of the potential used here may not be exact in the range of interactions we are talking about, any repulsive interaction sufficiently unscreened so that it falls slower than $1/r^{2/3}$, if not as $\ln r$, would still yield the same qualitative result.[17] It may be difficult to satisfy the conditions required to achieve this transition with currently known polymers. We look forward to more experimental work in this area, and also a better theoretical understanding of the predicted phase.

Acknowledgment. We are grateful for discussions with S. Fraden, R. Meyer, and D. Turnbull about the experimental situation. We also benefited from helpful comments by the referees. This research was supported by the National Science Foundation, in part by the MRSEC Program through Grant DMR-9400396 and through Grant DMR-9417047.

Appendix A: Path Integral Representation of the Partition Function

Z has the form of the path-integral representation of a matrix element of the time evolution operator $U = \exp(-iHt/\hbar) = \int D\mathbf{r}(t) \exp(iS[\mathbf{r}(t)])$ in quantum mechanics. Here, $S[\mathbf{r}(t)]$ is the action and z is the timelike variable, and the boundary conditions on the path represent the initial and final states. A Schröedinger-like partial differential equation for Z can be derived from this form, with a difference—in regular quantum mechanics, the highest time derivative that appears in S is $(d\mathbf{r}/dt)^2$, involving two derivatives, whereas in Z, we have $(d^2\mathbf{r}/dz^2)^2$ with four derivatives. So we need to specify not only $\mathbf{r}$, but also $d\mathbf{r}/dz \equiv \mathbf{v}$ at the two ends of the path. We thus have $Z(\mathbf{r},\mathbf{v};\mathbf{r}_o,\mathbf{v}_o;L)$: the partition function for a polymer of length L; coordinates $(\mathbf{r}_o, \mathbf{v}_o)$ at $z = 0$ and $(\mathbf{r}, \mathbf{v})$ at $z = L$. Many of the results of this section have also been derived by Le Doussal.[23]

Evolution in z represents adding another monomer at the end of the polymer. If the monomer length $l_o \ll l_P$, the evolution can be treated as continuous. For an infinitesimal addition l_o to L, we then have

$$Z(\mathbf{r},\mathbf{v};\mathbf{r}_o,\mathbf{v}_o;L+l_o) = \int d^2\mathbf{r} \int d^2\mathbf{v}\ \mathcal{T}(\mathbf{r},\mathbf{v};\mathbf{r}',\mathbf{v}';l_o)\, Z(\mathbf{r}',\mathbf{v}';\mathbf{r}_o,\mathbf{v}_o;L) \quad \text{(A1)}$$

where the transfer matrix is

$$\mathcal{T}(\mathbf{r},\mathbf{v};\mathbf{r}',\mathbf{v}';l_o) = \frac{\kappa}{2\pi T l_o} \exp\left\{-\frac{l_o}{T}\left[\frac{\kappa}{2}\left(\frac{\mathbf{v}-\mathbf{v}'}{l_o}\right)^2 + \frac{g}{2}\left(\frac{\mathbf{v}^2+\mathbf{v}'^2}{2}\right)^2 + \frac{k}{2}\left(\frac{\mathbf{r}^2+\mathbf{r}'^2}{2}\right)^2\right]\right\}\delta\left[\mathbf{r}-\mathbf{r}'-l_o\left(\frac{\mathbf{v}+\mathbf{v}'}{2}\right)\right] \quad \text{(A2)}$$

The normalization factor ensures that as $l_o \to 0$, $Z(L+l_o) \to Z(L)$.

Upon expanding Z on the left in l_o, and on the right in the changes in coordinates, we obtain the differential equation:

$$-T\frac{\partial Z}{\partial z} = \left(-\frac{T^2}{2\kappa}\nabla_{\mathbf{v}}^2 + T\mathbf{v}\cdot\nabla_{\mathbf{r}} + \frac{g}{2}\mathbf{v}^2 + \frac{k}{2}\mathbf{r}^2\right)Z \equiv \hat{H}Z \quad \text{(A3)}$$

A forming integration yields

$$Z(\mathbf{r},\mathbf{v};\mathbf{r}_o,\mathbf{v}_o;L) = \langle \mathbf{r},\mathbf{v}|e^{-\hat{H}L/T}|\mathbf{r}_o,\mathbf{v}_o\rangle = \sum_n \psi_n(\mathbf{r},\mathbf{v})\,\psi_n(\mathbf{r}_o,-\mathbf{v}_o)e^{-E_nL/T} \quad \text{(A4)}$$

where $\{\psi_n, E_n\}$ solve the eigenvalue equation for the "Hamiltonian" H. $\psi_n(\mathbf{r},-\mathbf{v})$, the "time"-reversed "wave function", is the equivalent of ψ_n^* in quantum mechanics.

In the limit of long "times" ($L \to \infty$), the "ground state" dominates the "evolution", and the free energy of fluctuations per unit length $f = (-T \ln Z)/L \simeq E_0$. The ground state wave function is of the form $\exp(-A\mathbf{v}^2 - B\mathbf{r}^2 + C\mathbf{v}\cdot\mathbf{r})$, with appropriate values of A, B, C, and E_0, giving

$$f = T\sqrt{\frac{2\sqrt{\kappa k}+g}{\kappa}} \quad \text{(A5)}$$

$\langle|\mathbf{r}|^2\rangle \equiv \langle\int dz\ \mathbf{r}^2(z)\rangle/L$ can be obtained as

$$\langle|\mathbf{r}|^2\rangle = -2T\frac{1}{Z}\frac{\partial Z}{\partial k} = 2\frac{\partial f}{\partial k} = \frac{T}{\sqrt{k(2\sqrt{\kappa k}+g)}} \quad \text{(A6)}$$

Similarly,

$$\langle|\mathbf{v}|^2\rangle = 2\frac{\partial f}{\partial g} = \frac{T}{\sqrt{\kappa(2\sqrt{\kappa k}+g)}} \quad \text{(A7)}$$

However, $\langle|\mathbf{r}''(z)|^2\rangle$ is not simply $2\partial f/\partial\kappa$ (which is negative), because the normalization factor in Z also involves κ, giving an extra contribution involving the small wavelength cutoff l_o. The sum of these three fluctuations is the fluctuation energy, $T\cdot L/l_o$.

Also of interest are the fluctuation correlation functions, such as

$$C(z) = \langle \mathbf{r}(0)\cdot\mathbf{r}(z)\rangle \quad \text{(A8)}$$

These are easily calculated in Fourier space:

$$\int dz\ \delta E[\mathbf{r}(z)] = \frac{1}{L}\sum_q \tilde{\epsilon}(q)|\tilde{\mathbf{r}}(q)|^2 \quad \text{(A9)}$$

where $\tilde{\mathbf{r}}(q) = \int dz\ \mathbf{r}(z)e^{iqz}$, $\tilde{\epsilon}(q) = \kappa q^4 + gq^2 + k$. By equipartition, $|\tilde{\mathbf{r}}(q)|^2 = TL/\tilde{\epsilon}(q) = S(q)$. $C(z)$ can then be calculated as $(1/L)\int(dq/2\pi)e^{-iqz}S(q)$. Its behavior will be dominated by the poles of $S(q)$, which could be complex or purely imaginary, depending on whether the dimensionless parameter $\alpha = g/2\sqrt{\kappa k}$ is $<$ or $>$ 1. The poles are at $q^* = \pm i/l_+ \pm 1/l_-$ where $l_\pm = 2\sqrt{\kappa/(2\sqrt{\kappa k} \pm g)}$.

For $\alpha < 1$, correlations decay exponentially over length l_+, oscillating with wavelength l_- as they do so:

$$\frac{C(z)}{\langle|\mathbf{r}|^2\rangle} = e^{-|z|/l_+}\left[\cos\frac{z}{l_-} + \frac{l_-}{l_+}\sin\frac{|z|}{l_-}\right] \quad \text{(A10)}$$

For $\alpha > 1$, correlations decay over a length $l = (l_+^{-1} - \bar{l}_-^{-1})^{-1}$ without oscillating:

$$\frac{C(z)}{\langle|\mathbf{r}|^2\rangle} = e^{-|z|/l_+}\left[\cosh\frac{z}{\bar{l}_-} + \frac{\bar{l}_-}{l_+}\sinh\frac{|z|}{\bar{l}_-}\right] \quad \text{(A11)}$$

with $\bar{l}_- = 2\sqrt{\kappa/(g-2\sqrt{\kappa k})}$.

A similar analysis in the Debye model would show that a distortion of in-plane wavelength $q_\perp$ applied to one face of the sample would experience oscillatory decay into the sample if $\alpha_1(q_\perp)$ (for a longitudinal deformation) or $\alpha_2(q_\perp)$ (for a transverse deformation) is <1, where $\alpha_{1,2}(q_\perp)$ are obtained by replacing $\Lambda_\perp$ in $\alpha_{1,2}$ of section IV by $q_\perp$.

This behavior reproduces that of a particle in a damping fluid with damping force $\gamma\mathbf{v}$, attached to a spring of spring constant K, experiencing a random force η (as in Brownian motion). If one took the particle mass $m = D\sqrt{\kappa}$, $\gamma = D\sqrt{2\sqrt{\kappa k}+g}$, $K = D\sqrt{k}$, and η to be Gaussian noise with $\langle\eta(t)\cdot\eta(t')\rangle = DT\delta(t-t')$ (again, $t \equiv z$), then one would recover the above results.

The continuum approximation breaks down at large g when $l_\pm \sim l_o$; one then has to work with the discretized version of the problem.

Appendix B: Validity of the Quadratic Approximation

In the quadratic model, the distribution of fluctuations about the minimum would be Gaussian. We have verified that it is very close to Gaussian for the full interaction potential by performing Monte Carlo simulations of a fluctuating polymer in the field of many stationary surrounding polymers, interacting via the pair potential 2.1.

The number of shells of neighbors to be included was determined by the condition that at the outermost shell, the interaction potential fell to a fraction, which we took to be 5%, of its value at the innermost shell. The polymer parameters were taken from B-DNA at room temperature:[19] $l_P = 600$ Å, $D = 20$ Å, and b was assumed to be 1.7 Å, close to its bare value, though it would be

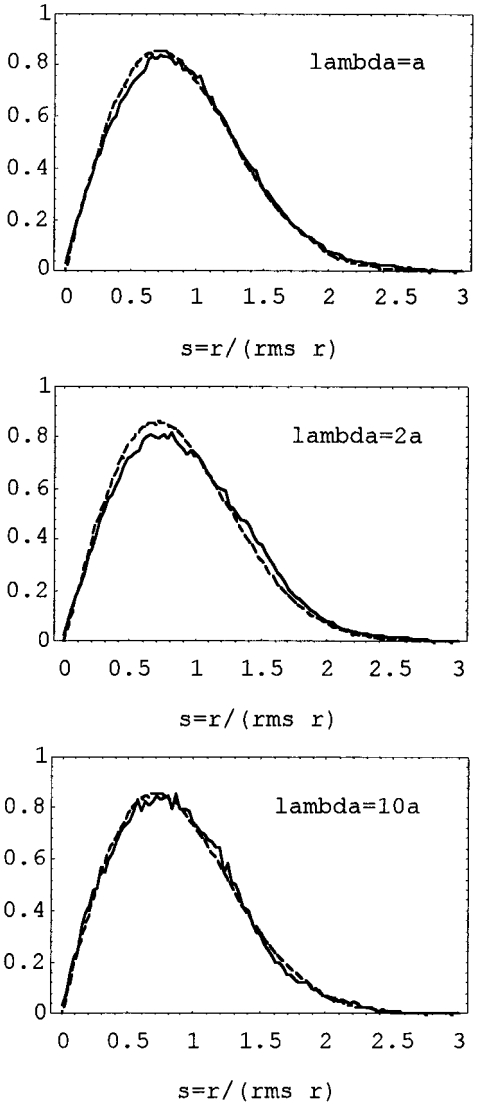

Figure 3. Distribution of segments of a polymer in radial displacement r from equilibrium, plotted as a function of $s = r/\sqrt{\langle|\mathbf{r}|^2\rangle}$. The Monte Carlo simulations of the Einstein model were performed for $\lambda = a$, $3a$, $10a$. The range of s shown was divided into 100 bins in calculating the distribution. Dotted lines show the theoretical quadratic distribution with variance $\langle|\mathbf{r}|^2\rangle$ as calculated within the Einstein model, not accounting for the <2% change due to discretization.

larger for finite c. We took $L = 2l_P$, which was many times l_{def}. The polymer was divided into $N = L/\Delta l$ segments of length Δl, and the energy was correspondingly discretized:

$$E(\{\mathbf{r}_n\}) = \Delta l \left[\frac{\kappa}{2}\sum_{n=1}^{N-1}\left(\frac{\mathbf{r}_{n+1} + \mathbf{r}_{n-1} - 2\mathbf{r}_n}{2\Delta l^2}\right)^2 + \frac{g}{2}\sum_{n=1}^{N}\left(\frac{\mathbf{r}_n - \mathbf{r}_{n-1}}{\Delta l}\right)^2 + \frac{k}{2}\sum_{n=0}^{N}\mathbf{r}_n^2\right] \quad \text{(B1)}$$

$\Delta l = l^*/4$ was chosen to balance the contributions from the bending energy ($\propto 1/\Delta l^3$) and the potential energy ($\propto \Delta l$).

The polymer was initialized in its equilibrium position $\mathbf{r}(z) = 0$ and allowed to thermalize for 2000 time steps, where each step involved a serial update of the segment positions using the Metropolis algorithm. The updated segment position was chosen within $d/4$ of the previous position, $d = \langle|\mathbf{r}|^2\rangle^{1/2}$ in the quadratic approximation, from eq 3.6. The distribution of the segments in r was then averaged over every fourth of the next 400 time steps, and divided into bins of size $\Delta r = 3d/100$. The parameter g describing an external field was set to 0. The results, compared with the expected quadratic distribution, are shown in Figure 3 and found to be in excellent agreement.

References and Notes

(1) Livolant, F.; Bouligand, Y. *J. Physique* **1986**, *47*, 1813. Livolant, F.; Levelut, A. M.; Doucat, J.; Benoit, J. P. *Nature* **1989**, *339*, 724.

(2) Podgornik, R.; Parsegian, V. A. *Macromolecules* **1990**, *23*, 2265 and references therein.

(3) Brezin, E.; Nelson, D. R.; Thiaville, A. *Phys. Rev. B* **1985**, *31*, 7124.

(4) Zeldov, E.; *et al. Nature* **1995**, *375*, 373.

(5) Fraden, S. F. In *Observation, Prediction and Simulation of Phase Transitions in Complex Fluids*; Baus, M., Rull, L. F., Ryckaert, J. P., Eds.; NATO ASI Series C; Kluwer Academic: The Netherlands, 1995; No. 460, p 113.

(6) Odijk, T. *Europhys. Lett.* **1993**, *24*, 177.

(7) Kwok, W. K.; *et al. Phys. Rev. Lett.* **1992**, *69*, 3370.

(8) Selinger, J. V.; Bruinsma, R. F. *Phys. Rev. A* **1991**, *43*, 2910. Note, however, that this approach predicts melting at densities such that the interpolymer spacing *exceeds* the hard core diameter.

(9) Nelson, D. R. In *Observation, Prediction and Simulation of Phase Transitions in Complex Fluids*; Baus, M.; Rull, L. F.; Ryckaert, J. P., Eds.; NATO ASI Series C; Kluwer Academic: The Netherlands, 1995; No. 460, p 293.

(10) Burkhardt, T. W. *J. Phys. A* **1995**, *28*, L629.

(11) Kleinert, H. *J. Math. Phys.* **1986**, *27*, 3003.

(12) Dodonov, V. V.; Klimov, A. B.; Man'ko, V. I. *Physica A* **1991**, *170*, 595.

(13) Schellman, J. A.; Stigter, D. *Biopolymers* **1977**, *16*, 1415. Stigter, D. *Ibid.* **1977**, *16*, 1435.

(14) Abramowitz, M.; Stegun, I. A. *Handbook of Mathematical Functions*; Dover: New York, 1972.

(15) Odijk, T. *Biophys. Chem.* **1993**, *46*, 69.

(16) Odijk, T. *Macromolecules* **1983**, *16*, 1340; **1984**, *17*, 502; **1986**, *19*, 2313.

(17) Nelson, D. R. Harvard University preprint.

(18) Helfrich, W.; Harbich, W. *Chem. Scr.* **1985**, *25*, 32.

(19) Podgornik, R.; Rau, D. C.; Parsegian, V. A. *Macromolecules* **1989**, *22*, 1780.

(20) Blatter, G.; *et al. Rev. Mod. Phys.* **1994**, *66*, 1125.

(21) Larkin, A. I. *Sov. Phys. JETP* **1970**, *31*, 784.

(22) Tang, J.; Fraden, S. *Biopolymers*, in press.

(23) Le Doussal, P. Unpublished work.

MA9608481